Optics & Laser Technology 180 (2025) 111519

Contents lists available at ScienceDirect

Optics and Laser Technology

journal homepage: www.elsevier.com/locate/optlastec

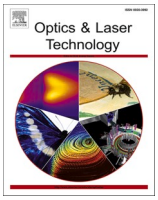

Polyphenylene oxide based lossy mode resonance fiber sensor for the detection of volatile organic and inorganic compounds

Sukanya Choudhary [a], Flavio Esposito [a,*], Lucia Sansone [b], Michele Giordano [b], Stefania Campopiano [a], Agostino Iadicicco [a,*]

[a] Department of Engineering, University of Naples "Parthenope", 80143 Naples, Italy
[b] Institute for Polymers, Composites and Biomaterials, National Research Council of Italy, IPCB-CNR, 80055 Portici, Italy

ARTICLE INFO

Keywords:
Gas sensors
Lossy mode resonance
Fiber optic sensors
Volatile organic compounds

ABSTRACT

This study presents the fabrication and characterization of a fiber optic gas sensor based on Lossy Mode Resonances (LMR). For the first time to our knowledge, a nanosized coating of polyphenylene oxide (PPO) is deposited on a cladding removed multimode silica fiber, serving both as the LMR supporting coating and sensitive overlay. The device exhibits a notable sensitivity of 2500 nm/RIU when immersed in glycerol-water based solutions. For gas detection, the PPO-based LMR device is exposed to varying concentrations of different volatile organic and inorganic compounds, including two alcohols (methanol and ethanol) and ammonia. The sensor demonstrates similar responses to methanol and ethanol gases with a sensitivity of about 0.56 nm/ppm and sensitivity of 0.25 nm/ppm to ammonia in the concentration range of 2.5–37.5 ppm, achieving limits of detection of a few ppm. To comprehensively evaluate the sensor performance, the investigation is also focused on the repeatability, reversibility, response times, as well as cross sensitivity to temperature and relative humidity.

1. Introduction

The demand for gas detectors has been steadily increasing for purposes focusing on safety being in industries and environmental concerns. Gas sensors play a role in averting accidents by detecting leaks and enabling quick responses to prevent potential dangers. Nowadays, the gas sensors must be integrated with the Internet-of-Things (IoTs). In this context, monitoring the levels of volatile organic compounds (VOC) as well as inorganic ones, is necessary to safeguard human health from exposure to concentrations, reducing the likelihood of respiratory problems or other health issues. Monitoring these compounds in enclosed spaces, like laboratories or manufacturing plants helps uphold a work environment. In manufacturing industries, like chemicals and pharmaceuticals, maintaining them under safe levels is crucial for production with high quality [1]. In general, gas sensing approaches are mainly based on the concurrence of two mechanisms. The first relies on the modification of the physical/chemical properties of a specific material, or combination of materials, like semiconductor metal oxides, polymers, and carbon nanotubes in form of thin film or bulk material, as consequence of the interaction, i.e. absorption or adsorption, with the gases under test. The second mechanism consists of an electrical or optical transducer able to detect the changes of the sensitive materials and convert them in an interpretable signal [2–4]. In this scenario, there is a large amount of gas sensor configurations which, in most of the cases, are classified according to the transducer mechanism [5–8]. Among them, in recent times fiber optic based sensors have gained much more importance because of unique characteristics including their ability for remote sensing, multiplexing capability, high sensitivity, durability and immunity to electromagnetic interferences, making them well suited for chemical detection applications in various industries [9–15]. In this scenario, the authors have demonstrated a gas sensor for the detection of liquefied petroleum gas and applied it in railway tunnel monitoring [16]. The sensor explored the well assessed optical fiber long period grating (LPG) technology coated by polymeric thin film, i.e. polystyrene, where the latter was tailored to induce the modal transition phenomenon [17].

Recently, between different fiber optic sensing platforms, there is a large interest on the phenomenon of Lossy Mode Resonances (LMR), since the publication of the first paper in 2010 [18]. In these configurations, thin films with high refractive index play a crucial role. Such coatings, once deposited on the fiber, changes the effective refractive index of the modes guided in the structure inducing wavelength

* Corresponding authors.
E-mail addresses: flavio.esposito@uniparthenope.it (F. Esposito), agostino.iadicicco@uniparthenope.it (A. Iadicicco).

https://doi.org/10.1016/j.optlastec.2024.111519
Received 7 May 2024; Received in revised form 10 July 2024; Accepted 24 July 2024
Available online 27 July 2024

selective attenuation bands in the fiber spectrum, due to the transition to guidance of some modes from core to thin film [19–21]. Some of the common thin film materials used to induce LMR are the metal oxides like indium tin oxide (ITO), titanium dioxide (TiO_2), tin dioxide (SnO_2), but recently also polymers have been employed for the purpose, including PAH, PAA, PSS, and PEI [22]. Although in 2019 the same phenomenon has been demonstrated on planar glass substate [23], the advantages of optical fiber sensing configurations make it still favourite in many applications. As matter of fact, many papers exploring the LMR based sensors for bio-sensing applications have been presented [24,25].

As far as LMR based gas sensors are concerned, most of them are fabricated on planar structures like coverslips. In [26], the authors reported about a chromium oxide (Cr_2O_3) thin film deposited onto a planar waveguide for LMR generation to detect ammonia down to a concentration of 10 ppbv. Graphene oxide (GO) has been also used for the purpose by the same authors in [27] for the detection of ethanol and acetone. Ethylene detection is instead provided in [28] for food and health monitoring using a coverslip coated with SnO_2 thin film. Finally, the same group investigated the combination of SnO_2 and a PEI/GO multilayer for the detection of 1-butanol [29]. So far, only a few works have focused on fiber optic configurations such as [30] and [31], where uncladded fiber coated with nanostructures of ITO and ZnO, respectively, were used for the detection of hydrogen and hydrogen sulfide. These works mainly focused on materials characterization. Finally, LMR device have been also employed for the measurement of relative humidity (RH) [32,33].

In this work, we report the fabrication and characterization of an LMR device for gas detection. It is based on a polymer layer, specifically polyphenylene oxide (PPO), which is deposited on the core of a cladding removed silica multimode optical fiber (MMF) with a double aim. The PPO thin film exhibits refractive index higher than silica one [34] making it suitable for the generation of LMRs. Based on our knowledge, it is the first time that such material has been employed for the purpose. Moreover, the exposure of the PPO coated device to certain gases, specifically VOCs like methanol and ethanol as well as inorganic ones like ammonia, results in a change in the refractive index of the polymer. This change affects the effective refractive indices of the overlay modes resulting in shifts in the LMR dips and enabling this technology in gas sensing fields: very few evidence of an LMR gas sensor based on a fiber optic configuration are now available. Sensitivity, repeatability, reversibility, and cross sensitivity to external parameters of the sensor have been evaluated demonstrating enhanced detection capabilities.

2. Materials and methods

2.1. Sensing material selection, synthesis and characterization

For the LMR supporting coating, a nanosized polymer layer of polyphenylene oxide or PPO has been employed. Such material has indeed a high refractive index of 1.6–1.7 [34] and a non-negligible absorption coefficient making it suitable for the generation of LMRs. This study stands unique in the literature as no prior work has explored LMRs with such kind of polymeric material [20]. Moreover, the affinity between the polymeric fiber coating makes the material a good candidate for the detection of volatile organic and inorganic compounds.

Regarding the material synthesis, PPO powder was purchased from Merck Life Science (Milano, Italy) and dissolved into a suitable solvent, i.e., chloroform to create a deposition solution, followed by stirring for approximately 30 min and a concentration of 9.3 % w/w has been selected.

Finally, to observe the morphology of PPO layer deposited on the optical fiber surface, SEM (Scanning Electron Microscope) images were taken by means of Quanta 200 FEG (FEI, USA) apparatus.

2.2. Optical fiber

A commercially available unconventional MMF model FG105LCA (Thorlabs, USA) with a 105/125 μm core/cladding diameter has been selected for the sensor. It is worth highlighting that the most of LMR based optical fiber devices involve MMF with larger core from 200 μm to 600 μm [20].

The sensing region of the fiber is further etched down to a diameter of about 95 μm to have guided modes sensitive to surroundings and further coated with nanosized polymer layer of polyphenylene oxide to generate LMRs. In this scenario, the polymer coating on the etched MMF alters the light guiding properties of the structure. In fact, LMR occurs when modes guided in the fiber core start experiencing a transition to guidance into the lossy thin film coating, leading to resonant dips in the transmission spectrum for those wavelengths at which the modes are near cut-off [35].

A schematic representation of the configuration is reported in Fig. 1. Specifically, the fabrication procedure involves that the standard MMF with a 105 μm core undergoes wet chemical etching using a 24 % HF solution to achieve the desired diameter of 95 μm, to completely remove the cladding and part of the core.

2.3. Experimental setup

2.3.1. Dip-coating approach

The PPO coating is deposited around the etched MMF region using a dip coating technique. Such technique ensures a uniform deposition of PPO, and the controlled withdrawal speed can influence the thickness of the coating. A dip coating bath is setup with a vertical translator, where the polymer PPO solution is poured into the dip coating bath. In the next step, etched fiber has been immersed in the solution and slowly withdrawn to induce solvent evaporation and further allowing the coated fiber to dry in a controlled environment to prevent dust or particle contamination with proper ventilation. In all cases, the deposition has been achieved by a single dip coating process. Notably, our approach distinguishes itself by employing a straightforward dip coating technique for fabricating the thin film layer at a room temperature in contrast to more intricate fabrication methods like sputtering, atomic layer deposition, and e-beam, our process emphasizes simplicity without compromising effectiveness.

The control of thickness of the coated layer is crucial to tune the LMR spectral features. It can be done acting mainly on solution concentration and withdrawal speed. In the following, we have reported the results achieved with the same PPO solution concentration of 9.3 % w/w and with different fiber withdrawal speed (1, 2, and 3 mm/s), i.e. different PPO layer thickness.

2.3.2. Optoelectronic setup

The interrogation setup for the measurement of the transmitted spectrum of the device is illustrated in Fig. 1, where one end of MMF is linked to a VIS optical source (Avantes AvaLight-HAL-S-Mini), while the other end is connected to a spectrometer operating in the visible range (Ocean Optics HR2000+).

2.3.3. Chamber for gas sensing test

The setup for testing is also schematically reported in Fig. 1, the sensor is placed inside a chamber with a volume of 70 mL, having an inlet to allow the gas to be injected and an outlet to allow the same to be removed from the chamber and expose the device to air. The testing procedure involves that each time different volumes containing saturated vapor of the target are injected into the chamber in order to reach a cumulative higher concentration, whereas the chamber is opened at the end of the experiment to expose the device to air. The climatic conditions of the chamber have been kept stabilized at 20 ± 0.5 °C of temperature and relative humidity of 48 ± 2 % during the measurements.

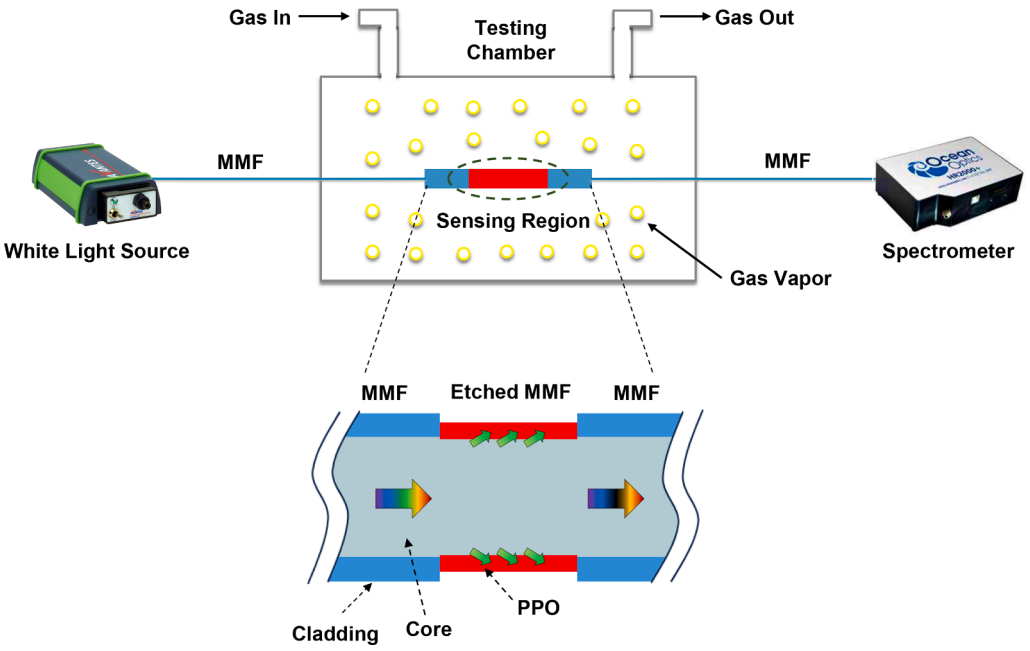

Fig. 1. Gas measurement setup and optoelectronic readout system, including schematic representation for fiber configuration of LMR device based on etched MMF with thin film coating of PPO.

3. Sensor fabrication and characterization

The fabrication procedure consists of a few steps following the approach reported in the previous section: i) etching of the MMF fiber via wet chemical procedure using HF at 24 % down to obtain a fiber diameter of 95 μm; and ii) deposition of the PPO thin film by dip-coating procedure.

3.1. Fiber preparation and deposition

Here we have reported the results regarding different devices using a 4 cm long etched MMF with 95 μm diameter, coated with PPO layer at a concentration of 9.3 % and different thickness achieved by tuning the fiber withdrawal speed during the dip-coating. The transmission spectral results are shown in Fig. 2(a) when the surrounding medium is air, obtained for extraction speeds of 3 mm/s, 2 mm/s and 1 mm/s, respectively.

Fig. 2 provides insights into how the thickness of polymer coating on the fiber affects the optical properties of the device and thereby tuning the LMR phenomena. As expected from dip-coating approach [36], the thickness of the deposited film increases with higher speed. Moreover, the thickness of the polymer coating affects the effective refractive index of the guided modes, in turn producing a resonance wavelengths shift. A thicker coating (depicted by blue line in plot) may lead to longer resonant wavelengths, i.e., around 900 nm, while a thinner coating (depicted by green line in plot) may result in shorter wavelengths, i.e., around 550 nm. Such behavior is completely in agreement with the theoretical working principle of LMR [19]. Moreover, this tunability allows to tailor the LMR phenomena to specific wavelengths of interest for different sensing applications. Thus, optimizing the deposition speed, i.e. the coating thickness, helps to achieve the desired LMR characteristics.

In the following, the sample achieved with a deposition speed of 1 mm/s is selected for further investigations. Fig. 3(a) and (b) illustrate SEM images of the morphology of the etched fiber coated with PPO layer at 1000x and 5000x magnification, respectively, where it is clearly visible that the PPO is uniformly coated around the optical fiber. As we are not able to provide a direct measurement of the PPO thickness, based on our previous experiments on polymer coated fiber devices [17] we can estimate that the resulting coating thickness is in a range of 100–500 nm.

Finally, in order to have an estimation of the ageing process of the device, the spectra were acquired again six months after the fabrication finding a wavelength shift not higher than 10 nm, confirming the good long-term stability of the material.

3.2. Characterization to surrounding refractive index changes

The spectral position of the generated resonance (LMR) is significantly dependent on the surrounding refractive index (SRI). Fig. 2(b) plots the same devices as Fig. 2(a) when they are immersed in water instead of air. Here, a large shift of about 120 nm and 160 nm, has been measured for the samples obtained at 1 mm/s and 2 mm/s, respectively, whereas in the case of 3 mm/s the band reaches out of the interrogation range.

In the following the sample achieved with a deposition speed of 1 mm/s was selected for further sensing characterization, as exemplary. The device has been immersed in glycerol-water solutions within the refractive index range of 1.33–1.38, and the corresponding wavelength shift in LMR band has been analyzed to obtain the characterization to surrounding refractive index changes.

In Fig. 4(a), illustrating the transmitted spectra of the device, the resonant wavelength of the LMR band in air is approximately 530 nm. Upon immersion in solutions with higher refractive indices, a noticeable red shift in the resonant wavelength occurred, ranging from 530 nm up to 780 nm, correlating with an increase in SRI as reported in Fig. 4(b). Such behavior resembles the typical trend with SRI of LMR devices [20]. Moreover, in Fig. 4(c) the attention is focused on the response between 1.33–1.38 highlighting a nearly linear trend with a high sensitivity of about 2500 nm/RIU, which underscores the remarkable potential of the device for chemical detection, emphasizing its applicability in highly sensitive detection scenarios. Such value is similar to other LMR based devices fabricated using metal oxides and other polymeric overlays achieved by different deposition methods, moreover it should be also highlighted that sensitivities even up to 4–5 times higher can be reached by employing materials with higher refractive index [19].

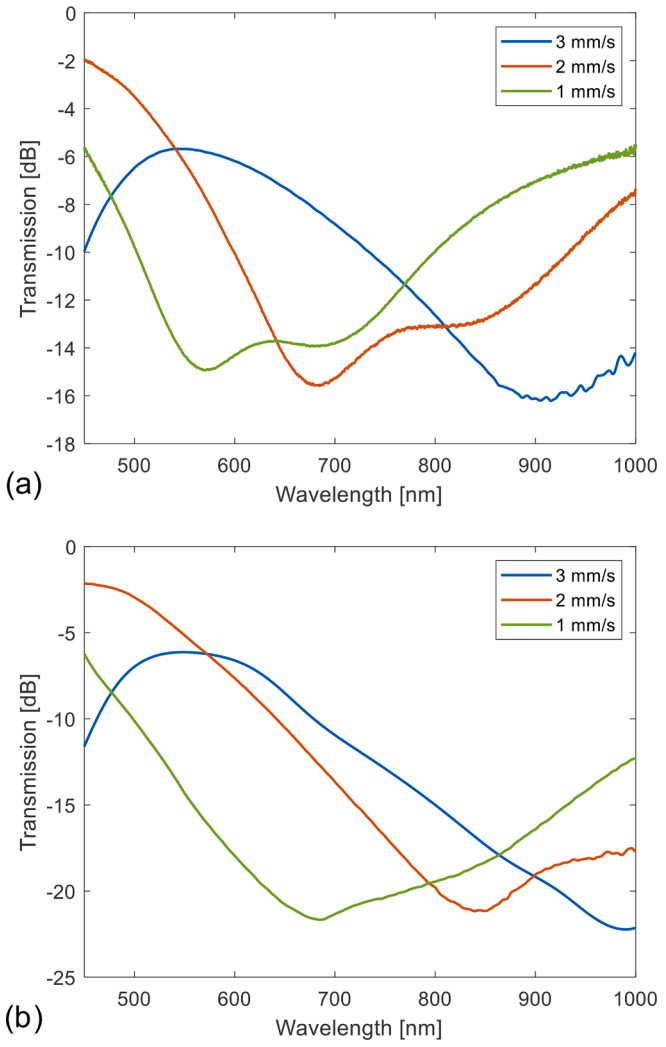

Fig. 2. (a) Transmission spectra of LMR devices with PPO layer achieved by different deposition speeds of 3 mm/s, 2 mm/s and 1 mm/s when the surrounding medium is air and (b) water, respectively.

4. Gas sensing results

4.1. Sensing of volatile compounds

Regarding the sensing mechanism that takes place when an LMR device coated with PPO is exposed for example to a gaseous target, it should be mentioned that the effective refractive indices of the waveguide modes change [37,38]. The sensing mechanism is governed by weak physical interactions such as electron transfer, and hydrogen bond formation [39].

In our initial investigation with methanol (CH_3OH) gas, the sensor response depicted a noticeable shift in resonant wavelength towards longer wavelengths, indicative of an increased refractive index in the PPO coating [19]. Real-time tracking of the sensor resonance wavelength is performed by fitting the minimum of the transmitted spectra through a second order polynomial fitting [40] and an acquisition time of 5 s is used. Specifically, a maximum resonant wavelength shifts of approximately 22 nm has been observed as the methanol gas concentration increased from concentration of 2.5 ppm to 37.5 ppm in steps of different concentration each time, as shown in Fig. 5(a). The LMR sensor exhibited proportional shifts corresponding to different methanol gas concentrations, revealing higher concentrations resulted in more extended resonant wavelength shifts. Post-exposure, the sensor spectra fully recovered, affirming the reversibility of the interaction.

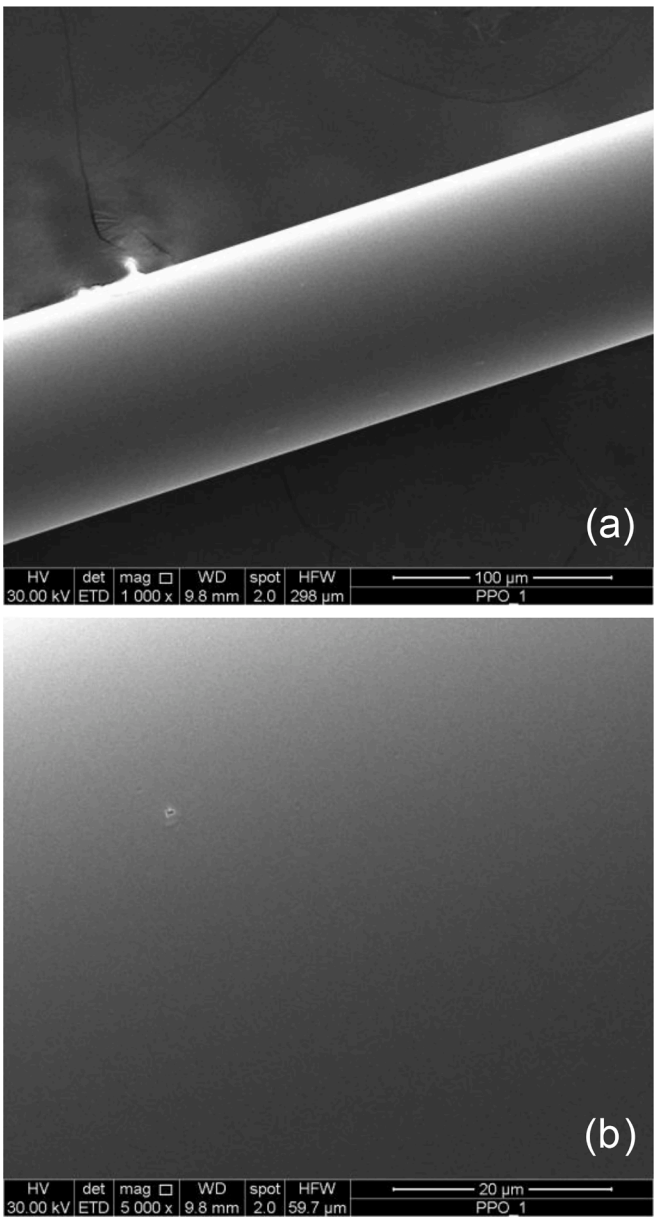

Fig. 3. SEM images of etched optical fiber coated with PPO layer at (a) 1000x and (b) 5000x magnification.

In the subsequent test involving ethanol (C_2H_5OH) gas, we observed that the sensor exhibited a response closely resembling that observed with methanol. Specifically, there is a notable maximum shift of approximately 22 nm in resonance wavelength corresponding to an increase in gas concentration from 2.5 ppm to 37.5 ppm as reported in Fig. 5(b). Also, in this case the response is reversible when the exposure to ethanol is terminated, and the device is surrounded by air. Based on results in this study, we found that LMR device showed similar responses to both methanol and ethanol gases. VOCs often have functional groups (e.g., hydroxyl, carbonyl) that can interact effectively with the polymer matrix of PPO: methanol and ethanol have indeed similar chemical structures as they both contain the hydroxyl (−OH) group bonded to a carbon atom [41].

Moreover, the device was also tested for the detection of ammonia (NH_3) vapors and the response is depicted in Fig. 5(c), where the maximum wavelength change in the range investigated is only about 10 nm. Therefore, a lower response is obtained in the case of ammonia, since it is a small, highly polar molecule, which can interact less strongly

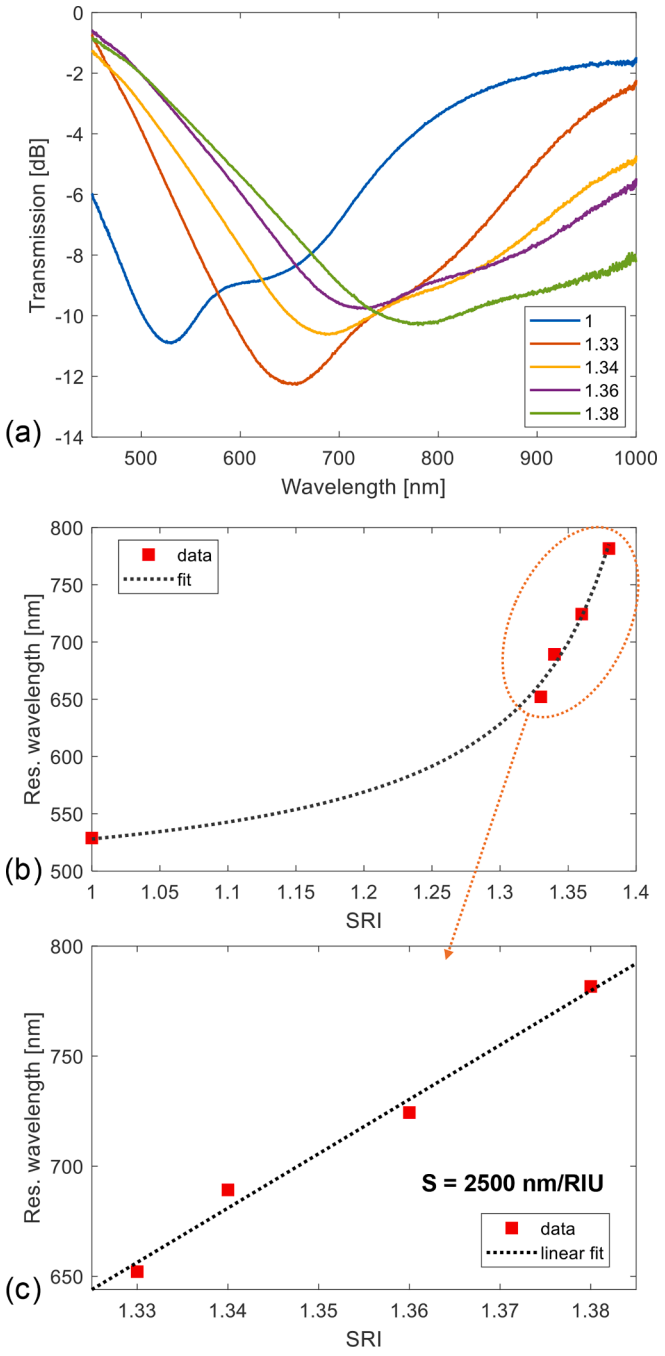

Fig. 4. (a) Transmission spectra of LMR device with PPO layer during SRI characterization upon immersion in different refractive index solutions ranging from 1.33 to 1.38; (b) Response of resonant wavelength shift with SRI and (c) corresponding linear trend in range 1.33–1.38 showcasing a sensitivity of 2500 nm/RIU.

with the hydrophobic PPO matrix [42].

Finally, Fig. 6 presents the calibration curves of the sensor, illustrating LMR wavelength shift data points plotted versus methanol, ethanol, and ammonia gas concentrations. Each measurement is reported in terms of mean value and error bars (accounting for three times the standard deviation), and the linear regression is represented by a dashed line. The responses to methanol and ethanol are similar, showing a maximum wavelength shift up to approximately 22 nm within concentration range 2.5–37.5 ppm, which defines the dynamic range of the sensor. A sensitivity S of 0.56 nm/ppm has been observed for both with an R^2 of 0.997 and 0.974 for methanol and ethanol, respectively. The

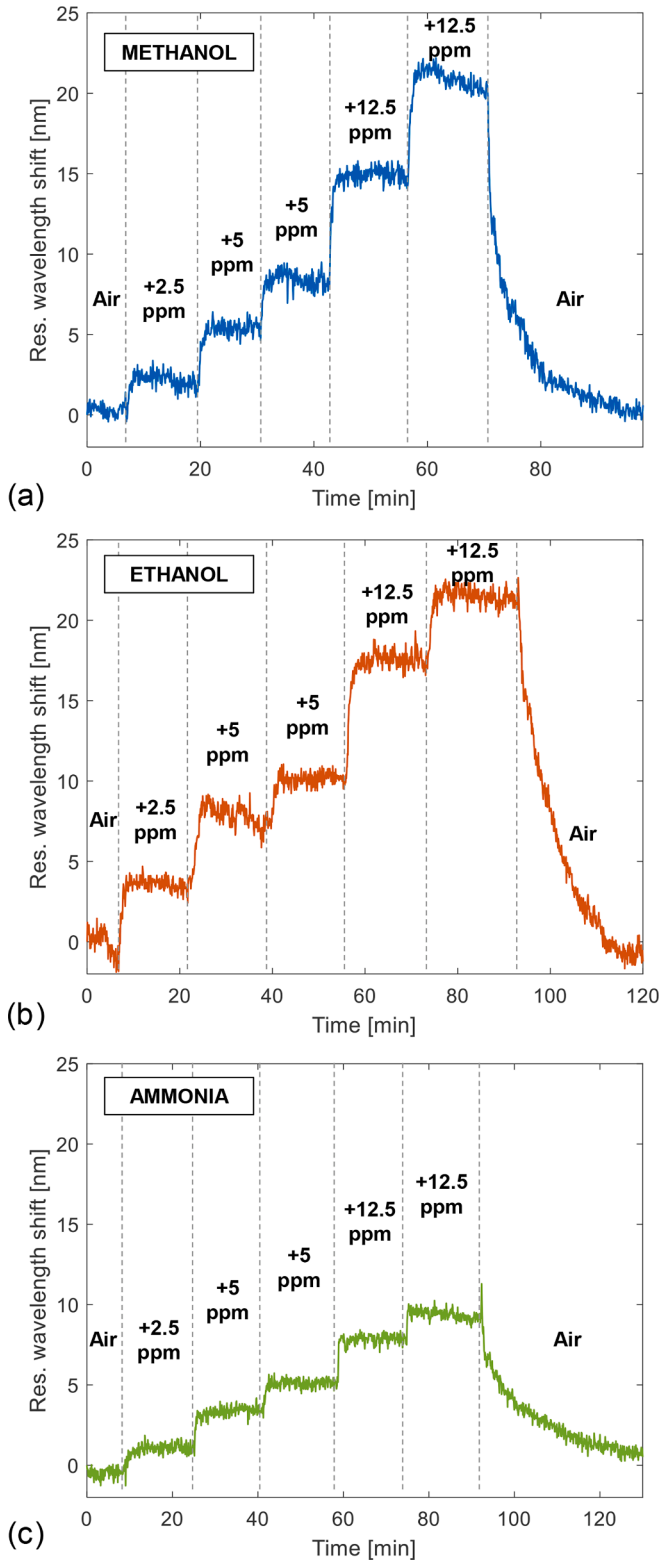

Fig. 5. Dynamic response of the LMR sensor to varying concentration of (a) methanol, (b) ethanol, and (c) ammonia. The vertical lines indicate the time instant when the concentration is changed.

limit of detection for these cases is 2 ppm using the 3σ/S method. Differently, for ammonia, the sensitivity is only 0.25 nm/ppm, with an R^2 of 0.939 and a limit of detection of 3 ppm. The response for methanol has been re-checked after six months, yielding similar results and demonstrating a good long term-stability of the sensor performance.

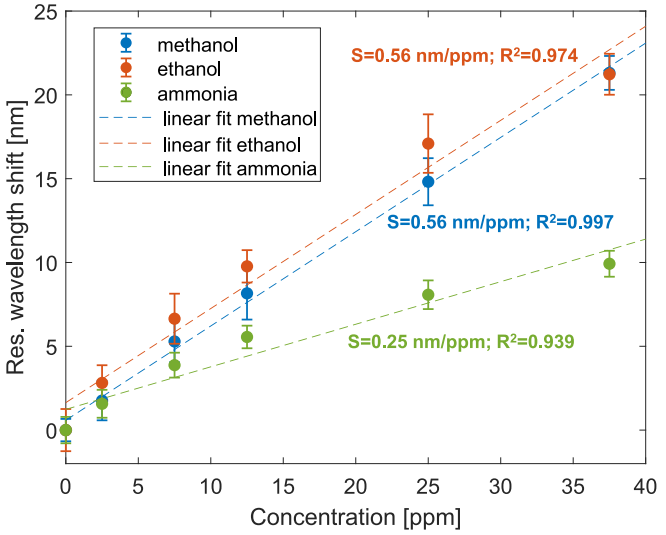

Fig. 6. Calibration curves of the sensor reporting shift in resonant wavelength with respect to gas concentration of methanol, ethanol and ammonia.

4.2. Repeatability, recovery, and response time

Different tests have been also performed to see the repeatability and recovery of the measurements utilizing our sensor, as depicted in Fig. 7 (a), illustrating the response to three different methanol exposures at 12.5 ppm. Here the resonance wavelength shifts observed are approximately 6 nm in each case demonstrating a good repeatability. Moreover, it can be clearly observed that after each exposure the response returns to its original state when the device is put in air, showing a full recovery.

Remarkably, the sensor exhibited a swift response time, defined as the interval between 10 % and 90 % of the sensor response, at a mere 60 s as can be seen in Fig. 7(b). The recovery time, measured from 90 % to 10 % of the sensor response during the recovery phase, is established to be 10 min in Fig. 7(b). It is important to highlight that the reaction phase duration also encompasses the time required for the target to leave the chamber. Such response and recovery times are in agreement with the literature [27,28].

4.3. Cross sensitivity to temperature and relative humidity

In our investigation we further evaluated the cross sensitivities to environmental parameters of temperature and relative humidity (RH).

The response of the device to temperature changes in the range 25–45 °C is reported in Fig. 8(a), where the wavelength shift decreases with increasing temperature, exhibiting a linear trend with a slope of −0.8 nm/°C. Such behavior agrees with the fact that it is expected that the refractive index of the polymeric layer decreases with increasing temperature. Moreover, such trend is in agreement with literature on metal oxide based LMR sensors, for which a lower value was found [43]. The LMR device can be thus employed together with a fiber Bragg grating for the temperature measurement and subsequent compensation [43].

Finally, the response of the gas sensor to RH changes has been investigated and found to be only around 1.5 nm for a change in relative humidity in range 48–70 % (i.e., a ΔRH=22 %), as reported in Fig. 8(b). Based on these results, the sensor performance remains stable and reliable, with minimal interference from varying humidity levels. This observation underscores the sensor robustness and suitability for applications where accurate gas detection is crucial, regardless of ambient humidity conditions. Our findings contribute to a deeper understanding of the sensor capabilities and its potential for deployment in diverse environmental settings.

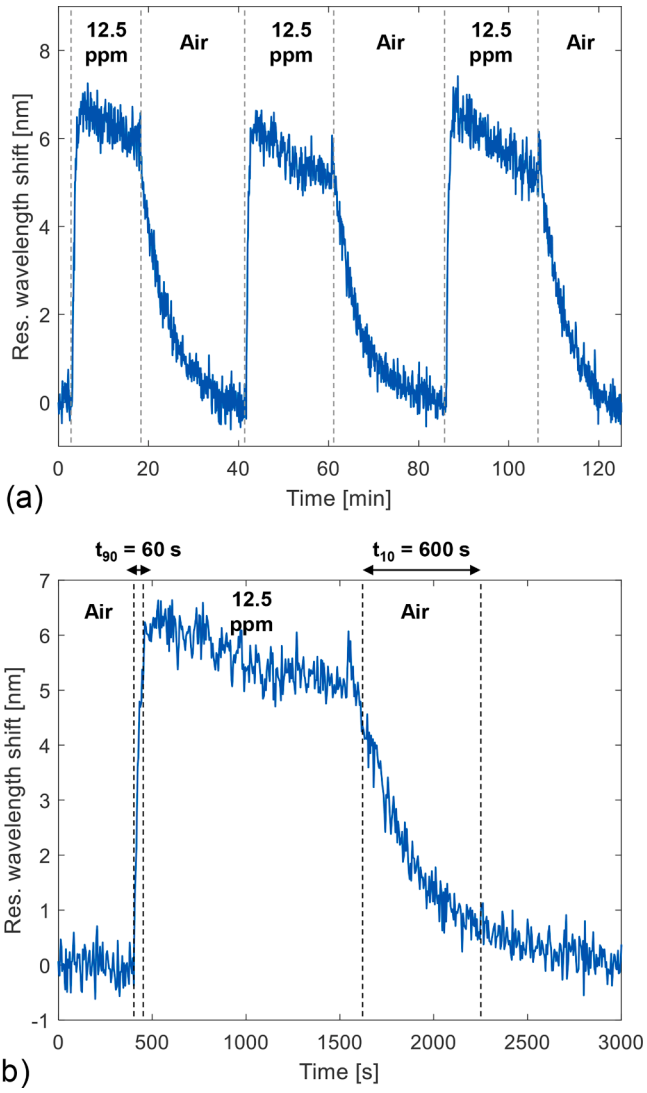

Fig. 7. Dynamic response of LMR device to same 12.5 ppm concentration of methanol gas: (a) for three consecutive cycles for repeatability; (b) for one cycle illustrating response and recovery time of 60 s and 600 s, respectively.

4.4. Comparison of the performance and future perspectives

If compared to other LMR sensors from literature, in our case the test has been performed at lower concentrations of ethanol with a significant response, as also summarized in Table 1.

Moreover, if compared to other techniques for gas detection (such as metal oxide and electrochemical sensors, colorimetric tubes, gas chromatography), optical fiber based LMR gas sensors can have higher or similar sensitivity, do not require bulky instrumentation, are immune to electromagnetic interference and can work in difficult-to-access areas and harsh environments; however, in current state, they may still require specialized knowledge for setup and interpretation which demands further investigation for transition from research to market [1,2].

The results confirm the possibility to measure different hazardous substances to be employed in a variety of applications, such as air quality monitoring, breath detection, leak detections, food control, chemical and biological research, agriculture, railway industry, etc [1].

Finally, in order to improve the selectivity of the PPO-based sensors, the polymer matrix can be modified with nanoparticles, metal oxides, or other polymers. For example, doping PPO with metal oxides like ZnO or TiO_2 can create additional active sites for VOC adsorption, significantly enhancing the sensor sensitivity [42].

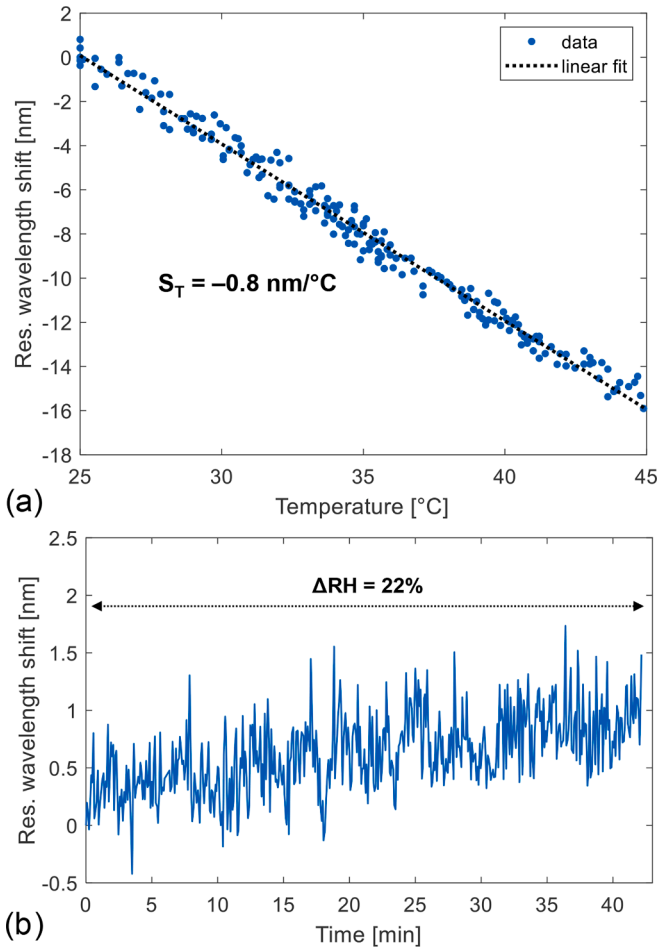

Fig. 8. Response of LMR device to: (a) temperature changes in range 25–45 °C; and (b) relative humidity changes in range 48–70 %.

Table 1
Comparison of the performance of LMR based gas sensors.

Sensor configuration	Analyte target	Concentration range	Ref.
Planar waveguide with Cr_2O_3	Ammonia	10–70 ppbv	[26]
Planar waveguide with GO	Ethanol, Acetone	600–2020 ppm, 1600-6390 ppm	[27]
Planar waveguide with SnO_2	Ethylene	16–66 ppm	[28]
Planar waveguide with SnO_2 and PEI/GO	1-butanol	250–1750 ppm	[29]
Uncladded fiber with ITO and ITO NPs	Hydrogen	10–100 ppm	[30]
Uncladded fiber with ZnO and ZnO NRs	Hydrogen sulfide	10–100 ppm	[31]
Uncladded fiber with PPO	Methanol, Ethanol, Ammonia	2.5–37.5 ppm	This work

5. Conclusions

We have reported the results concerning a fiber optic gas sensor utilizing LMR phenomenon, detailing its fabrication and characterization. Notably, it marks the first instance, to the best of our knowledge, of applying a nanosized polyphenylene oxide (PPO) coating on a cladding removed MMF to induce such phenomena; and it represents one of the few examples of an LMR gas sensor integrated in a fiber optic setup. This coating serves dual purposes, acting as both the supporting layer for LMR and the sensitive overlay. The sensor demonstrates significant refractometric sensitivity, registering 2500 nm/RIU when submerged in glycerol-water solutions. For gas detection, the device is exposed to varying concentrations of volatile organic and inorganic compounds, such as methanol, ethanol, and ammonia. The exposure of the PPO coated sensor to specific gases, triggers a change in the polymer refractive index, which in turn impacts the waveguide effective refractive indices, leading to shifts in the LMR dips. The sensor exhibits comparable responses to alcohols (methanol and ethanol), showing a sensitivity of approximately 0.56 nm/ppm within the concentration range of 2.5–37.5 ppm and a limit of detection of 2 ppm. Differently, in the case of ammonia, a sensitivity of 0.25 nm/ppm in the same range has been obtained with a limit of detection of 3 ppm. We have conducted evaluations to assess sensitivity, repeatability, reversibility, and cross-sensitivity to environmental parameters, demonstrating improved detection capabilities.

CRediT authorship contribution statement

Sukanya Choudhary: Writing – original draft, Investigation. **Flavio Esposito:** Writing – original draft, Investigation, Conceptualization. **Lucia Sansone:** Writing – review & editing, Resources, Investigation. **Michele Giordano:** Supervision, Conceptualization. **Stefania Campopiano:** Supervision, Conceptualization. **Agostino Iadicicco:** Writing – review & editing, Supervision, Conceptualization.

Declaration of competing interest

The authors declare that they have no known competing financial interests or personal relationships that could have appeared to influence the work reported in this paper.

Data availability

Data will be made available on request.

Acknowledgements

The work of Flavio Esposito was supported by the D.M. 1062/2021 - FSE REACT EU - PON Ricerca e Innovazione 2014-2020 - Azione IV.4 “Dottorati e contratti di ricerca su tematiche dell’innovazione” under contract nr. 41-I-15372-1 CUPI65F21001200001.

References

[1] M. Khatib, H. Haick, Sensors for Volatile Organic Compounds, ACS Nano. 16 (2022) 7080–7115, https://doi.org/10.1021/acsnano.1c10827.
[2] S. Dhall, B.R. Mehta, A.K. Tyagi, K. Sood, A review on environmental gas sensors: Materials and technologies, Sensors Int. 2 (2021) 100116, https://doi.org/10.1016/j.sintl.2021.100116.
[3] S.M. Majhi, A. Mirzaei, H.W. Kim, S.S. Kim, T.W. Kim, Recent advances in energy-saving chemiresistive gas sensors: A review, Nano Energy. 79 (2021) 105369, https://doi.org/10.1016/j.nanoen.2020.105369.
[4] X. Wang, O.S. Wolfbeis, Fiber-Optic Chemical Sensors and Biosensors (2015–2019), Anal. Chem. 92 (2020) 397–430, https://doi.org/10.1021/acs.analchem.9b04708.
[5] X. Liu, S. Cheng, H. Liu, S. Hu, D. Zhang, H. Ning, A Survey on Gas Sensing Technology, Sensors. 12 (2012) 9635–9665, https://doi.org/10.3390/s120709635.
[6] H. Ji, W. Zeng, Y. Li, Gas sensing mechanisms of metal oxide semiconductors: a focus review, Nanoscale. 11 (2019) 22664–22684, https://doi.org/10.1039/C9NR07699A.
[7] J. Hodgkinson, R.P. Tatam, Optical gas sensing: a review, Meas. Sci. Technol. 24 (2013) 012004, https://doi.org/10.1088/0957-0233/24/1/012004.
[8] Z. Wang, W. Zhang, X. Liu, M. Li, X. Lang, R. Singh, C. Marques, B. Zhang, S. Kumar, Novel Optical Fiber-Based Structures for Plasmonics Sensors, Biosensors. 12 (2022) 1016, https://doi.org/10.3390/bios12111016.
[9] Y. Zhao, Y. Liu, B. Han, M. Wang, Q. Wang, Y. Zhang, Fiber optic volatile organic compound gas sensors: A review, Coord. Chem. Rev. 493 (2023) 215297, https://doi.org/10.1016/j.ccr.2023.215297.

[10] F. Esposito, (INVITED)Chemical sensors based on long period fiber gratings: A review, Results Opt. 5 (2021) 100196, https://doi.org/10.1016/j.rio.2021.100196.
[11] C. Elosua, I.R. Matias, C. Bariain, F.J. Arregui, Volatile organic compound optical fiber sensors: A review, Sensors. 6 (2006) 1440–1465, https://doi.org/10.3390/s6111440.
[12] I. Dominguez, J.M. Corres, I. Del Villar, J.D. Mozo, R. Simerova, P. Sezemsky, V. Stranak, M. Śmietana, I.R. Matias, Electrochemical lossy mode resonance for detection of manganese ions, Sensors Actuators B Chem. 394 (2023) 134446, https://doi.org/10.1016/j.snb.2023.134446.
[13] M. Li, R. Singh, Y. Wang, C. Marques, B. Zhang, S. Kumar, Advances in Novel Nanomaterial-Based Optical Fiber Biosensors—A Review, Biosensors. 12 (2022) 843, https://doi.org/10.3390/bios12100843.
[14] W. Zhang, R. Singh, Z. Wang, G. Li, Y. Xie, R. Jha, C. Marques, B. Zhang, S. Kumar, Humanoid shaped optical fiber plasmon biosensor functionalized with graphene oxide/multi-walled carbon nanotubes for histamine detection, Opt. Express. 31 (2023) 11788, https://doi.org/10.1364/OE.486844.
[15] X. Liu, R. Singh, G. Li, C. Marques, B. Zhang, S. Kumar, WaveFlex Biosensor-Using Novel Tri-Tapered-in-Tapered Four-Core Fiber With Multimode Fiber Coupling for Detection of Aflatoxin B1, J. Light. Technol. 41 (2023) 7432–7442, https://doi.org/10.1109/JLT.2023.3301069.
[16] F. Esposito, A. Zotti, G. Palumbo, S. Zuppolini, M. Consales, A. Cutolo, A. Borriello, S. Campopiano, M. Zarrelli, A. Iadicicco, Liquefied Petroleum Gas Monitoring System Based on Polystyrene Coated Long Period Grating, Sensors. 18 (2018) 1435, https://doi.org/10.3390/s18051435.
[17] F. Esposito, A. Zotti, R. Ranjan, S. Zuppolini, A. Borriello, S. Campopiano, M. Zarrelli, A. Iadicicco, Single-Ended Long Period Fiber Grating Coated With Polystyrene Thin Film for Butane Gas Sensing, J. Light. Technol. 36 (2018) 825–832, https://doi.org/10.1109/JLT.2017.2776599.
[18] I. Del Villar, C.R. Zamarreno, M. Hernaez, F.J. Arregui, I.R. Matias, Lossy Mode Resonance Generation With Indium-Tin-Oxide-Coated Optical Fibers for Sensing Applications, J. Light. Technol. 28 (2010) 111–117, https://doi.org/10.1109/JLT.2009.2036580.
[19] I. Del Villar, F.J. Arregui, C.R. Zamarreño, J.M. Corres, C. Bariain, J. Goicoechea, C. Elosua, M. Hernaez, P.J. Rivero, A.B. Socorro, A. Urrutia, P. Sanchez, P. Zubiate, D. Lopez, N. De Acha, J. Ascorbe, I.R. Matias, Optical sensors based on lossy-mode resonances, Sensors Actuators, B Chem. 240 (2017) 174–185, https://doi.org/10.1016/j.snb.2016.08.126.
[20] F. Chiavaioli, D. Janner, Fiber Optic Sensing With Lossy Mode Resonances: Applications and Perspectives, J. Light. Technol. 39 (2021) 3855–3870, https://doi.org/10.1109/JLT.2021.3052137.
[21] N. Paliwal, J. John, Lossy Mode Resonance (LMR) Based Fiber Optic Sensors: A Review, IEEE Sens. J. 15 (2015) 5361–5371, https://doi.org/10.1109/JSEN.2015.2448123.
[22] I. Vitoria, C. Ruiz Zamarreño, A. Ozcariz, I.R. Matias, Fiber Optic Gas Sensors Based on Lossy Mode Resonances and Sensing Materials Used Therefor: A Comprehensive Review, Sensors. 21 (2021) 731, https://doi.org/10.3390/s21030731.
[23] O. Fuentes, I. Del Villar, J.M. Corres, I.R. Matias, Lossy mode resonance sensors based on lateral light incidence in nanocoated planar waveguides, Sci. Rep. 9 (2019) 8882, https://doi.org/10.1038/s41598-019-45285-x.
[24] F. Chiavaioli, D. Santano Rivero, I. Del Villar, A.B. Socorro-Leránoz, X. Zhang, K. Li, E. Santamaría, J. Fernández-Irigoyen, F. Baldini, D.L.A. van den Hove, L. Shi, W. Bi, T. Guo, A. Giannetti, I.R. Matias, Ultrahigh Sensitive Detection of Tau Protein as Alzheimer's Biomarker via Microfluidics and Nanofunctionalized Optical Fiber Sensors, Adv. Photonics Res. 3 (2022) 2200044, https://doi.org/10.1002/adpr.202200044.
[25] M. Śmietana, M. Koba, P. Sezemsky, K. Szot-Karpińska, D. Burnat, V. Stranak, J. Niedziółka-Jönsson, R. Bogdanowicz, Simultaneous optical and electrochemical label-free biosensing with ITO-coated lossy-mode resonance sensor, Biosens. Bioelectron. 154 (2020) 112050, https://doi.org/10.1016/j.bios.2020.112050.
[26] D. Armas, P. Zubiate, C. Ruiz Zamarreno, I.R. Matias, Ammonia Gas Optical Sensor Based on Lossy Mode Resonances, IEEE Sensors Lett. 7 (2023) 1–4, https://doi.org/10.1109/LSENS.2023.3301843.
[27] I. Vitoria, E.E. Gallego, S. Melendi-Espina, M. Hernaez, C. Ruiz Zamarreño, I. R. Matías, Gas Sensor Based on Lossy Mode Resonances by Means of Thin Graphene Oxide Films Fabricated onto Planar Coverslips, Sensors. 23 (2023) 1459, https://doi.org/10.3390/s23031459.
[28] E.E.G. Martínez, M.H. Otamendi, C.R. Zamarreño, I.R. Matías, LMR-Based Optical Sensor for Ethylene Detection at Visible and Mid-Infrared Regions, IEEE Sensors Lett. 7 (2023) 1–4, https://doi.org/10.1109/LSENS.2023.3297371.
[29] E.E.G. Martínez, I.R. Matías, S. Melendi-Espina, M. Hernáez, C.R. Zamarreño, Lossy mode resonance based 1-butanol sensor in the mid-infrared region, Sensors Actuators B Chem. 388 (2023) 133845, https://doi.org/10.1016/j.snb.2023.133845.
[30] S.K. Mishra, S.P. Usha, B.D. Gupta, A lossy mode resonance-based fiber optic hydrogen gas sensor for room temperature using coatings of ITO thin film and nanoparticles, Meas. Sci. Technol. 27 (2016) 045103, https://doi.org/10.1088/0957-0233/27/4/045103.
[31] S.P. Usha, S.K. Mishra, B.D. Gupta, Zinc oxide thin film/nanorods based lossy mode resonance hydrogen sulphide gas sensor, Mater. Res. Express. 2 (2015) 095003, https://doi.org/10.1088/2053-1591/2/9/095003.
[32] P.J. Rivero, A. Urrutia, J. Goicoechea, F.J. Arregui, Optical fiber humidity sensors based on Localized Surface Plasmon Resonance (LSPR) and Lossy-mode resonance (LMR) in overlays loaded with silver nanoparticles, Sensors Actuators B Chem. 173 (2012) 244–249, https://doi.org/10.1016/j.snb.2012.07.010.
[33] D.L. Bohorquez, I. Del Villar, J.M. Corres, I.R. Matias, Generation of lossy mode resonances in a broadband range with multilayer coated coverslips optimized for humidity sensing, Sensors Actuators B Chem. 325 (2020) 128795, https://doi.org/10.1016/j.snb.2020.128795.
[34] J.F. Wall, J.C. Brumfield, R.W. Murray, E.A. Irene, Spectroscopic Ellipsometry and Atomic Force Microscopy of Polyphenylene Oxide Films, J. Electrochem. Soc. 141 (1994) 306–310, https://doi.org/10.1149/1.2054706.
[35] J.M. Corres, I. Del Villar, F.J. Arregui, I.R. Matias, Analysis of lossy mode resonances on thin-film coated cladding removed plastic fiber, Opt. Lett. 40 (2015) 4867, https://doi.org/10.1364/OL.40.004867.
[36] D. Grosso, How to exploit the full potential of the dip-coating process to better control film formation, J. Mater. Chem. 21 (2011) 17033, https://doi.org/10.1039/c1jm12837j.
[37] D. Liu, R. Kumar, F. Wei, W. Han, A.K. Mallik, J. Yuan, S. Wan, X. He, Z. Kang, F. Li, C. Yu, G. Farrell, Y. Semenova, Q. Wu, High sensitivity optical fiber sensors for simultaneous measurement of methanol and ethanol, Sensors Actuators B Chem. 271 (2018) 1–8, https://doi.org/10.1016/j.snb.2018.05.106.
[38] A. Prasanth, S.R. Meher, Z.C. Alex, Experimental analysis of SnO2 coated LMR based fiber optic sensor for ethanol detection, Opt. Fiber Technol. 65 (2021) 102618, https://doi.org/10.1016/j.yofte.2021.102618.
[39] O.Y. Posudievsky, N.V. Konoschuk, A.L. Kukla, A.S. Pavluchenko, Y.M. Shirshov, V. D. Pokhodenko, Comparative analysis of sensor responses of thin conducting polymer films to organic solvent vapors, Sensors Actuators B Chem. 151 (2011) 351–359, https://doi.org/10.1016/j.snb.2010.07.049.
[40] S. Choudhary, F. Esposito, L. Sansone, M. Giordano, S. Campopiano, A. Iadicicco, Lossy Mode Resonance Sensors in Uncoated Optical Fiber, IEEE Sens. J. 23 (2023) 15607–15613, https://doi.org/10.1109/JSEN.2023.3280675.
[41] L. Liao, W. Ruan, M. Zhang, M. Lin, Recent Progress in Modification of Polyphenylene Oxide for Application in High-Frequency Communication, Materials (basel). 17 (2024) 1086, https://doi.org/10.3390/ma17051086.
[42] G. Chowdhury, Advances in the Development of Modified Polyphenylene Oxide Membranes for Gas Separation Applications, in: Polyphenylene Oxide Modif. Polyphenylene Oxide Membr., Springer US, Boston, MA, 2001: pp. 105–147. doi: 10.1007/978-1-4615-1483-1_4.
[43] J.J. Imas, C.R. Zamarreño, I. Del Villar, J.C.C. Da Silva, V. Oliveira, I.R. Matías, Optical fiber thermo-refractometer, Opt. Express. 30 (2022) 11036, https://doi.org/10.1364/OE.450316.